The Electronic Journal of Mathematics and Technology, Volume 19, Number 1, ISSN 1933-2823

Billiards: At the intersection of Physics, Geometry and Computer Algebra Systems

José A. Vallejo
jvallejo@mat.uned.es
Departmento de Matemáticas Fundamentales
Universidad Nacional de Educación a Distancia
Spain

Abstract

We study the properties of billiards (mainly elliptical) as dynamical systems, in particular, their integrability, and the existence and computation of periodic orbits. An implementation of the involved computations in a free CAS (Maxima) is also presented, as a tool for visualization and experimentation, which can be useful in web-based courses and distance learning.

1 Introduction

In a realistic setting, even the simplest question about the motion in a billiard can be difficult to solve. For instance, starting with a ball at (x_0, y_0), kicked with initial velocity (v_x, v_y), we may ask: 'Will the ball hit the table at the fixed but otherwise randomly chosen position (x, y) before 10^6 rebounds?' In general, the answer will be 'No', because there is a loss of energy when rolling and impacting on the table, so after a few rebounds the ball will stop, probably without reaching the goal point. Thus, we must assume that energy is conserved, so the motion of the ball continues indefinitely. Now the problem is that the only way we can answer, is following the ball's trajectory from the starting point, maybe along a really large number of rebounds. It is not feasible to try to answer armed just with pencil and paper, so we go for a computer and write a program to construct the trajectory given the data (x_0, y_0) and (v_x, v_y), using Newton's equations. We are then modeling the billiard as a dynamical system. Here we face the following problem: The computer can store the intermediate values of the position only up to a certain precision. This fact will influence the answer depending on whether the system is chaotic or not. In the first case, sensitivity on initial conditions will render our answer useless: Our prediction will depend on the precision used to describe the dynamics, and each rebound will amplify the initial errors committed in determining positions. Therefore, we need to be sure about the chaotic character of our billiard before we start to play.

It turns out that the chaotic character of a billiard depends on its shape. To be precise, rectangular and elliptical billiards determine integrable dynamical systems, hence their dynamics are regular. But other polygons or smooth boundaries, give rise to non-integrable, chaotic systems (indeed, there is

a conjecture by Birkhoff [2] stating that among all the billiards whose shape is given by a smooth, convex curve, only the elliptic case is integrable). We will explore what can be said about the motion in this case, and what kind of questions about it make sense, trying to keep the mathematics (and the physics) at a level as elementary as possible. In doing so, we will see that billiards provide an excellent environment for blending Classical Mechanics, Mathematics (Calculus, Geometry) and the use of Computer Algebra Systems (CAS). The possibility of numerically and visually experimenting with a concrete physical system, makes this an interesting tool, well suited for distance learning and self-study.

In this paper, we use the CAS Maxima (`https://maxima.sourceforge.io`), but everything here can be easily adapted to any other CAS. Some general references for dynamical systems are [1], [9], [12], for billiards see [7], [11], [13]. To save space, this paper does not include the source code of all the functions used in the text, only the main functions are shown in Section 6 (full code is available upon request).

2 Dynamical Systems and their integrability

For us, a dynamical system will be any physical system Σ that can be modeled using Newton's equations. A *configuration* will be any point in $\mathbb{R}^N$, where $N \in \mathbb{N}$. A given system will not be able to attain any arbitrary configuration. The allowed configurations fill up a submanifold $\Gamma \subset \mathbb{R}^N$ called the *configuration space*, and the dimension $r = \dim \Gamma$ is called the number of *degrees of freedom* of the system.

The time evolution of Σ will be described by a smooth map $\mathbf{x} : I \subset \mathbb{R} \to \Gamma \subset \mathbb{R}^N$, carrying t to $\mathbf{x}(t)$, where I is an interval containing $0 \in \mathbb{R}$. Newton's equation are then written as $m\frac{\mathrm{d}^2\mathbf{x}}{\mathrm{d}t^2}(t) = \mathbf{F}(\mathbf{x}(t))$, where $\mathbf{F} : \Gamma \subset \mathbb{R}^N \to \mathbb{R}^N$ is the *force field* (notice that, unless otherwise explicitly stated, we are going to consider only *autonomous*, velocity-independent forces). Defining the *linear momentum* $\mathbf{p} = m\mathrm{d}\mathbf{x}/\mathrm{d}t$ this is also equivalent to $\frac{\mathrm{d}\mathbf{p}}{\mathrm{d}t}(t) = \mathbf{F}(\mathbf{x}(t))$.

Example 1 *Here $N = 1$ and $\Gamma = \mathbb{R}$. We assume that the motion is determined by a potential $V(x)$, so $x : I \subset \mathbb{R} \to \mathbb{R}$ satisfies Newton's equation $m\ddot{x} = -\nabla V(x) = -V'(x)$ (In the sequel, we will use points over a letter to denote derivatives with respect to time t). More precisely, for each $t \in I \subset \mathbb{R}$ we have a configuration $x(t) \in \mathbb{R}$, and the curve $t \mapsto x(t)$ satisfies the ordinary differential equation $m\ddot{x} = -V'(x(t))$. This is an example of one-dimensional motion.* △

We now introduce two important classes of systems: the conservative and the integrable ones. They both have in common the existence of conserved quantities of the motion.

2.1 Conservative systems

Consider the case of a time-independent force which comes from a potential function $V \in \mathcal{C}^\infty(\Gamma)$. Thus, we have

$$m\ddot{x}(t) = -\nabla V(\mathbf{x}(t))\,. \tag{1}$$

These systems form a particular class, called *conservative systems*. The reason is that a certain function, called the *energy*, is conserved along their motion.

To explain this fact, we need to introduce some more terminology. Recall that the allowed configurations form the configuration space $\Gamma \subset \mathbb{R}^N$, now we are going to introduce a space containing configurations *and* momenta, the so called *phase space*. Generally speaking[1] this space is just $M = \Gamma \times \mathbb{R}^N \subset \mathbb{R}^{2N}$ (but see the footnote at the beginning of the next subsection). Each trajectory on configuration space, $\mathbf{x} : I \subset \mathbb{R} \to \Gamma \subset \mathbb{R}^N$, determines another curve on phase space, called its *lifting*, denoted $\tilde{\mathbf{x}}$ and acting as $\tilde{\mathbf{x}}(t) = (\mathbf{x}(t), \mathbf{p}(t))$.

Remark 2 *The points on phase space $M \subset \mathbb{R}^{2N}$ are called the* states *of Σ. They can be identified with the set of initial conditions for Newton's equations; thus, each state uniquely determines the evolution of the system (by the existence and uniqueness theorems for ordinary differential equations).*

For a conservative system, there exists a function on phase space $E : M \to \mathbb{R}$ such that its composition with the lifting of the actual trajectory $\mathbf{x}(t)$ is a constant mapping. This function, called the *total energy* of Σ, is defined as $E(\mathbf{x}, \mathbf{y}) = \frac{1}{2} m \langle \mathbf{y}, \mathbf{y} \rangle + V(\mathbf{x})$, where $\langle \cdot, \cdot \rangle$ is the Euclidean scalar product on $\mathbb{R}^N$, and $V : \Gamma \subset \mathbb{R}^N \to \mathbb{R}$ is the potential.

Theorem 3 (Conservation of Energy) *For any trajectory $\mathbf{x} : I \subset \mathbb{R} \to \Gamma \subset \mathbb{R}^N$ (that is, a solution of Newton's equations (1)), we have $\frac{\mathrm{d}}{\mathrm{d}t}(E \circ \tilde{\mathbf{x}})(t) = 0$.*

The proof is just a direct computation using the chain rule and equations (1).

Example 4 (One-dimensional motion) *For any* conservative *system in one dimension, the trajectory $x : I \subset \mathbb{R} \to \Gamma \subset \mathbb{R}$ must satisfy $\varepsilon = E(x, m\dot{x}) = \frac{1}{2} m \dot{x}(t)^2 + V(x(t))$ for some constant $\varepsilon \in \mathbb{R}$. Then, we can solve for $\dot{x}$ to obtain $\dot{x}(t) = \sqrt{2(\varepsilon - V(x))/m}$. Moreover, recalling the inverse function theorem, applied to $t = t(x)$, we get (in the region $\varepsilon > V(x)$ bounded by the* turning points*, that is, those configurations for which the velocity is zero, $\dot{x}(t) = 0$): $\frac{\mathrm{d}t}{\mathrm{d}x} = 1/\sqrt{\frac{2}{m}(\varepsilon - V(x))}$. Therefore, we can compute $t = t(x)$ by means of an integration:*

$$t = \int \frac{\mathrm{d}x}{\sqrt{\frac{2}{m}(\varepsilon - V(x))}},$$

and once the relation $t = t(x)$ is explicitly determined, we can invert it to get $x = x(t)$ if needed. Thus, we get the following important fact: for one-dimensional systems, the existence of one conserved quantity (the energy) leads to the solution of the equations of motion by a quadrature (the computation of an integral). We say that one-dimensional conservative systems are integrable. △

2.2 Integrable systems

We have just seen that one-dimensional conservative systems are integrable. How about higher dimensional systems? To answer this question, think of the motion not taking place in configuration space, but on phase space M. This is a $2r-$dimensional space, where r is the number of degrees of freedom[2]. If we have a set of n functions *on phase space* which are conserved quantities, $f_1, \ldots, f_n$,

[1] That is, in absence of non-holonomic constraints.

[2] We have $r = \dim \Gamma$ and M defined as $M = \Gamma \times \mathbb{R}^N$, but the factor $\mathbb{R}^N$ can actually be replaced by $\mathbb{R}^r$ because velocities must be tangent to $\Gamma \subset \mathbb{R}^N$.

then the motion will occur on the intersection $M(c_1,\dots,c_n) = M \cap f_1^{-1}(\{c_1\}) \cap \cdots \cap f_n^{-1}(\{c_n\})$, where $c_1,\dots,c_n$ are some real constants.

The dimension of this intersection (as a submanifold of M) is $2r-n$. There are some possibilities here. For instance, in the most favorable case in which $n = 2r-1$, the dimension of this intersection (as a submanifold of M) will be exactly 1, that is, we will have the motion restricted to a curve which must be the solution we are looking for. In Example 4, $r = 1 = N$, so the phase space was $2-$dimensional. The existence of just one conserved quantity defined on phase space, the energy, restricts the motion to the solution curve $x(t)$. This kind of systems, with r degrees of freedom and $n = 2r-1$ independent conserved quantities defined on phase space (also called *first integrals* or simply *integrals of the motion*)[3], are called *maximally superintegrable*.

When the system Σ has r degrees of freedom and exactly $n = r$ independent first integrals, we say that it is *integrable*, and *superintegrable* if the number n of independent first integrals satisfies $r < n < 2r-1$.

Example 5 (Central forces) *A force acting on a particle is called a* central force *if its supporting line (the line along which it acts on bodies) passes through a fixed point O, which is then called the* center *of the force. Thus, if we denote by $\mathbf{r}(t)$ the position of the particle at instant $t \in I \subset \mathbb{R}$ as measured from O, so we get the curve in configuration space $\mathbf{r}(t) = \overline{O\mathbf{x}(t)}$, we will have $\mathbf{F}(\mathbf{r}(t)) = f(\mathbf{r}(t))\mathbf{e_r}$, with $f : \Gamma \subset \mathbb{R}^N \to \mathbb{R}$ a smooth function and $\mathbf{e_r}$ the unit vector in the direction of $O\mathbf{x}(t)$ (we omit the time dependence to avoid overloading the notation).*

When describing the motion under the action of a central force, the notion of angular momentum is crucial. The angular momentum *with respect to a point $P \in \mathbb{R}^N$ of a particle of mass m, described by the trajectory $\mathbf{x}(t)$, is defined as the function* on phase space *given by $\mathbf{L}_P(\mathbf{x},\mathbf{y}) = \overline{P\,\mathbf{x}} \times \overline{P\,\mathbf{y}}$. Thus, if we consider the lifting of the curve $\mathbf{x}(t)$ to phase space, and evaluate the angular momentum on it, writing $\mathbf{L}_P(t) = \mathbf{L}_P(\mathbf{x}(t), m\dot{\mathbf{x}}(t))$ for the composition, we get $\mathbf{L}_P(t) = m\overline{P\mathbf{x}(t)} \times \overline{P\dot{\mathbf{x}}(t)}$. In the case of central forces we obviously take $P = O$, yielding the more common expression $\mathbf{L}(t) = m\mathbf{r}(t) \times \dot{\mathbf{r}}(t)$.*

A straightforward computation shows that, when the force is central, $\dot{\mathbf{L}}(t) = 0$, that is: the angular momentum is a first integral in any central-force system. Hence, central-force systems (with $r = 3$ degrees of freedom) are superintegrable (as the three components of $\mathbf{L}$ are conserved independently)[4]. △

The motion of integrable systems is *regular* and *stable*. Under very mild conditions, precisely stated in the so-called Arnold-Liouville-Mineur (ALM) theorem, the trajectories on phase space are bounded and either periodic or quasi-periodic. In any case, small deviations from the initial conditions yield new trajectories remaining close to the original ones for some time (actually, two initially close trajectories will diverge linearly in time [4]). This feature survives when projecting down to configuration space: no chaos is possible in integrable systems.

More precisely, a geometric interpretation of the ALM theorem is this: When a system is integrable, it admits a special class of coordinates, called *action-angle coordinates*; when the system is

[3] Some additional assumptions are needed in order to guarantee that these integrals are functionally independent, that is, the intersections above effectively define a submanifold with reduced dimension, but we will not care about these details here, and we will simply assume that all the required conditions are satisfied.

[4] In fact, these systems are maximally superintegrable, due to the existence of an additional first integral provided by the Laplace-Runge-Lenz vector, which only has one independent component, giving a total of $5 = 2 \cdot 3 - 1$ integrals of motion.

expressed in terms of these, its phase space becomes foliated by tori. Each torus is labeled by a particular value of the action coordinate J (for $r = 2$), and on that torus, the motion is linear, parameterized by the angle coordinate θ. Figure 1 (taken from [8]) illustrates the aspect that phase space adopts in a typical integrable system.

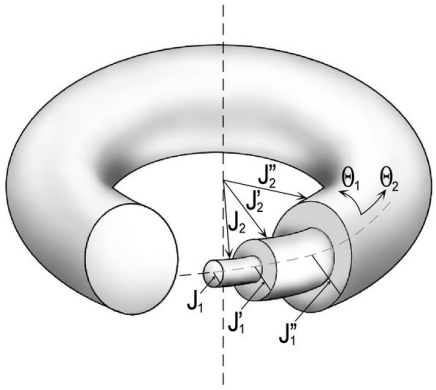

Figure 1: Foliation of phase-space by tori

3 Billiards

There are some properties common to all billiards considered as dynamical systems. Fist of all, as mentioned in the Introduction, we consider that the collisions of the ball on the boundary occur without exchanging energy (*elastic collisions*), so we have a conserved quantity. Being a two-dimensional system, every time there exists another first integral the billiard under consideration will be integrable.

The next observation is that the impact force acts along the normal to the boundary at the point of impact, in absence of friction. This property alone, allows us to deduce many important consequences that characterize the simplest cases of rectangular and circular billiards. One of them is the reflection law.

Theorem 6 (Reflection law) *In a billiard collision, the angle of reflection equals the angle of incidence.*

Example 7 (A rectangular billiard) *In this case, the hypothesis of elastic collisions means that energy (equivalently, v^2) is conserved, and the reflection law, taking into account the changes of orientation occurring at the boundary, implies that the absolute value of the horizontal component of velocity, $|v_x|$, is conserved too (in fact, both $|v_x|$ and the vertical component $|v_y|$ are conserved). The rectangular billiard is integrable, hence not chaotic.* △

3.1 Circular billiards. The Poncelet porism

The next case to consider is that of a circular billiard. Here, the forces along the normal of the boundary always point radially, that is, they are directed toward the geometric center of the circumference: We have a central force problem. Thus, aside from the energy we have another conserved quantity, angular momentum $\mathbf{L}$ (recall Example 5). This system is also integrable, not chaotic.

For circular billiards, some interesting phenomena begin to appear. Take a Cartesian coordinate system centered at the geometric origin of the billiard O, and consider the ball departing from a point $\mathbf{z}$ inside the billiard with a certain velocity, and reaching the boundary at point $\mathbf{P}$. Some point $\mathbf{x}_0$ on the segment $\overline{\mathbf{zP}}$ will be the orthogonal projection of the center O, that is, the line $\overline{\mathbf{zP}}$ will be tangent to the circle with center O and radius $\|\mathbf{x}_0\|$. Also, if the ball incides on $\mathbf{P}$ forming an angle θ_0 with respect to the line containing $\overline{O\mathbf{P}}$, it will rebound with an angle $-\theta_0$ with respect to the same line $\overline{O\mathbf{P}}$; thus, after running a distance $\|\overline{\mathbf{x}_0\mathbf{P}}\|$ along the new direction, it will touch again the inner circumference with center O and radius $\|\mathbf{x}_0\|$, $S_{\mathbf{x}_0}(O)$. This reasoning applies without changes after each rebound, so the trajectory of the ball is such that each straight segment part of it, is tangent to the circumference $S_{\mathbf{x}_0}(O)$ (see Figure 2, where the trajectory starting from a point on the bisector line, with coordinates $(2r/9, 2r/9)$ and initial angle 0.469π, r being the radius of the circumpherence, is shown after 50 rebounds).

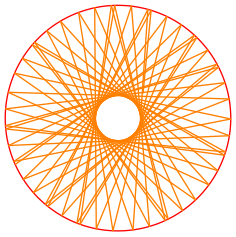

Figure 2: Caustics in a circular billiard

Due to this property, that circumference is called the *caustic* of the trajectory (geometrically, it is just the envelope).

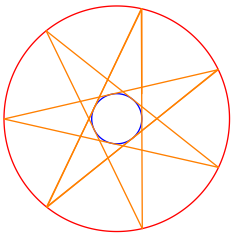

Figure 3: Closed trajectories in a circular billiard

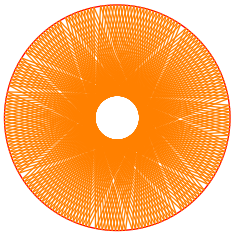

Figure 4: Non-closed trajectories in a circular billiard

The trajectory in Figure 2 is not closed. One could wonder whether there exists closed trajectories or not, so let us try with a different initial angle. Figure 3 shows the result of taking the same initial point but with initial angle (with respect to the horizontal) $\pi/2$, after 50 iterations. The caustic is drawn in blue. For a generic trajectory, though, we get a non-closed orbit; the first example considered, that of an initial angle 0.469π, gives the graph in Figure 4 after 200 iterations.

Notice, however, that none of these trajectories is *dense*: the inner region bounded by the caustic is never crossed. It turns out that there exists a close relation between caustics and closed orbits on any billiard with perimeter determined by a conic, due to a classical result on Projective Geometry discovered by J. V. Poncelet (1822).

Theorem 8 (Poncelet porism) *Consider two confocal conics $\mathcal{C}_{inn}$ and $\mathcal{C}_{out}$. Take a point $\mathbf{p}_0$ on the outer conic $\mathcal{C}_{out}$ and draw a line from it, tangent to the inner conic $\mathcal{C}_{inn}$. Determine the point of intersection of this line with the outer conic, and call it $\mathbf{p}_1$. Repeat this procedure with $\mathbf{p}_1$ as the starting point, instead of $\mathbf{p}_0$, and consider the resulting trajectory. If it is closed after n rebounds, then any other trajectory similarly constructed will be closed after n rebounds. In other words, given that a single closed polygonal trajectory exists, all other trajectories sharing the same caustic will be closed, with the same period.*

There are many proofs of this theorem available. Perhaps the most accessible is the one in [6]. The reasoning given at the beginning of this subsection proves the theorem for the particular case of concentric circles. In 3.2 we will present the proof of a weaker result valid when the outer conic is an ellipse.

Remark 9 *The existence of the caustic, and its forbidden interior, can be physically interpreted in terms of the conservation of angular momentum. Recall that $\mathbf{L} = \mathbf{r} \times \mathbf{v}$. Hence, its norm is $L = rv \sin\alpha$, where α is the angle between $\mathbf{r}$ and $\mathbf{v}$. As $\mathbf{L}$ lies on the normal to the billard's plane, its direction is constant and so the fact that is conserved translates into the constancy of L as well. We can write, then $\sin\alpha = L/rv = C/r$, with $C > 0$ constant. The trigonometric bound $\sin\alpha \leq 1$ then yields $r \geq C$. We have considered the degenerate case of a circular billiard (where the caustics are also circles), but as we will see, Poncelet porism can also be physically interpreted in the elliptic case.*

3.2 Elliptic billiards

In this section all vectors will be considered three-dimensional. To this end, consider that the ellipse describing the billiard lies on the $z = 0$ plane.

Continuing with more complicated shapes, we now analyze elliptic billiards. Suppose the boundary is given by an ellipse of major semiaxis a, and minor semiaxis b. Let $\mathbf{f} = (\sqrt{a^2 - b^2}, 0, 0)$ be the position of one of the foci, and $-\mathbf{f}$ that of the other. If $\mathbf{r}(t)$ denotes the position of the ball at the instant t, define the focal distances (see Figure 3) $\mathbf{r}_1(t) = \mathbf{r}(t) - \mathbf{f}$ and $\mathbf{r}_2(t) = \mathbf{r}(t) + \mathbf{f}$.

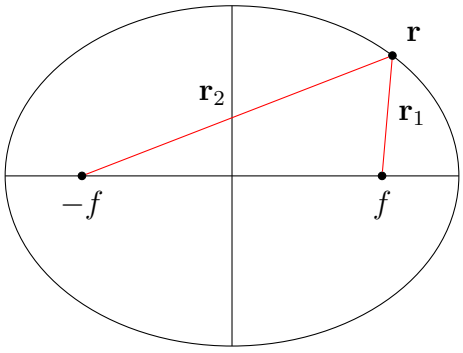

Figure 5: Ellipse geometry

The following result implies (because we already have a first integral, the energy) that an elliptic billiard is an integrable system.

Theorem 10 *The function $I = \langle \mathbf{L}_1, \mathbf{L}_2 \rangle$, where $\mathbf{L}_i(t) = \mathbf{r}_i(t) \times \mathbf{v}(t)$ (for $1 \leq i \leq 2$) and $\mathbf{v}(t) = \dot{\mathbf{r}}(t)$ is the velocity, is a first integral of the motion.*

The proof is a long but straightforward computation, which is best done introducing elliptic coordinates (ξ, η) in the plane of the ellipse, defined in terms of the Cartesian coordinates (x, y) as $x = f \cosh \xi \cos \eta$, and $y = f \sinh \xi \sin \eta$.

The computation of the angular momenta $\mathbf{L}_1$, $\mathbf{L}_2$ from $\mathbf{r}_1 = (x - f, y, 0)$, $\mathbf{r}_2 = (x + f, y, 0)$ and $\mathbf{v}$, leads to that of

$$I = \langle \mathbf{L}_1, \mathbf{L}_2 \rangle = f^4(\cosh^2 \xi - \cos^2 \eta)(-\sin^2 \eta \cdot \dot{\xi}^2 + \sinh^2 \xi \cdot \dot{\eta}^2)\,. \tag{2}$$

It is clear that this expression does not change under the transformation occuring at the point of impact, $(\dot{\xi}, \dot{\eta}) \mapsto (-\dot{\xi}, \dot{\eta})$, hence the theorem follows.

The next (purely geometric) result, taken from [11], tells us what the caustics of an elliptic billiard are.

Theorem 11 *A billiard trajectory inside an ellipse forever remains tangent to a fixed confocal conic. More precisely, if a segment of a billiard trajectory does not intersect the segment $\overline{F_1F_2}$, then all the segments of this trajectory do not intersect $\overline{F_1F_2}$ and are all tangent to the same ellipse with foci F_1 and F_2; and if a segment of a trajectory intersects $\overline{F_1F_2}$, then all the segments of this trajectory intersect $\overline{F_1F_2}$ and are all tangent to the same hyperbola with foci F_1 and F_2.*

Proof. Let $\overline{A_0A_1}$ and $\overline{A_1A_2}$ be consecutive segments of a billiard trajectory, see Figure 6. Assume that $\overline{A_0A_1}$ does not intersect the segment $\overline{F_1F_2}$ (the other case is dealt with similarly). It follows from the reflection law (Theorem 6), that the angles made by segments $\overline{F_1A_1}$ and $\overline{F_2A_1}$ with the ellipse are equal. Likewise, the segments $\overline{A_0A_1}$ and $\overline{A_2A_1}$ make equal angles with the ellipse. Hence the angles $\angle A_0A_1F_1$ and $\angle A_2A_1F_2$ are equal. Reflect F_1 in $\overline{A_0A_1}$ to point F_1', and F_2 in $\overline{A_1A_2}$ to F_2'. Let B be the intersection point of the lines $\overline{F_1'F_2}$ and $\overline{A_0A_1}$, and C of the lines $\overline{F_2'F_1}$ and $\overline{A_1A_2}$. Consider

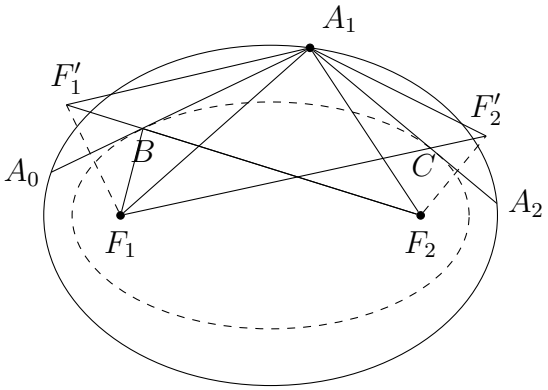

Figure 6: Caustics in an elliptic billiard

the ellipse $\mathcal{E}_1$ with foci F_1 and F_2 that is tangent to the line $\overline{A_0A_1}$. Since the angles $\angle F_2BA_1$ and $\angle F_1'BA_0$ are equal, and so are the angles $\angle F_1'BA_0$ and $\angle F_1BA_0$, the angles $\angle F_2BA_1$ and $\angle F_1BA_0$ are equal. Again by the reflection law, the ellipse $\mathcal{E}_1$ touches $\overline{A_0A_1}$ at the point B. Likewise the ellipse

$\mathcal{E}_2$ with foci F_1 and F_2 touches $\overline{A_1A_2}$ at the point C. We want to show that these two ellipses coincide or, equivalently, that $|\overline{F_1B}|+|\overline{BF_2}| = |\overline{F_1C}|+|\overline{CF_2}|$, which is reduced to $|\overline{F_1'F_2}| = |\overline{F_1F_2'}|$. Notice that the triangles $\triangle F_1'A_1F_2$ and $\triangle F_1A_1F_2'$ are congruent. Indeed, $|\overline{F_1'A_1}| = |\overline{F_1A_1}|$ and $|\overline{F_2A_1}| = \overline{F_2'A_1}|$ by symmetry. In addition, the angles $\angle F_1'A_1F_2$ and $\angle F_1A_1F_2'$ are equal: the angles $\angle A_0A_1F_1$ and $\angle A_2A_1F_2$ are equal, hence so are the angles $\angle F_1'A_1F_1$ and $\angle F_2'A_1F_2$, and adding the common angle $\angle F_1A_1F_2$ implies that $\angle F_1'A_1F_2 = \angle F_1A_1F_2'$. Equality of the triangles $\triangle F_1'A_1F_2$ and $\triangle F_1A_1F_2'$ implies that $|\overline{F_1'F_2}| = \overline{F_1F_2'}|$, which had to be proven. ■

As an immediate consequence of this theorem, we have for elliptic billiards the same relation between caustics and closed orbits that we found in the circular case, namely: Given that a single closed polygonal trajectory exists, all other trajectories sharing the same caustic will be closed, with the same period.

There is also an interpretation of Theorem 11 in terms of integrals of motion. Let our elliptic table be given by its semiaxes a, b. The constant-coordinates grid defined by the elliptic coordinates can be described by the one-parameter set of confocal conics

$$\frac{x^2}{a^2+\lambda} + \frac{y^2}{b^2+\lambda} = 1 \tag{3}$$

where the original ellipse corresponds to $\lambda = 0$, for values $\lambda \in]-b^2, +\infty[$ we get a family of ellipses sharing their foci, and for $\lambda \in]-a^2, b^2[$ we have a family of confocal hyperbolae orthogonal to that of the ellipses.

Suppose now that the initial segment of a trajectory is tangent to one of these constant-coordinate curves. Can we tell which one is going to be? If the segment is described by the equation $y = mx+c$, the tangency condition means that there exists a point (x_0, y_0) belonging to both curves, the line $y = mx + c$ and a certain member of the family (3), yielding the system

$$\begin{cases} \dfrac{x_0^2}{a^2+\lambda} + \dfrac{y_0^2}{b^2+\lambda} = 1 \\ y_0 = mx_0 + c\,. \end{cases}$$

After some algebraic manipulations, we get $(m^2+1)\lambda = c^2 - b^2 - m^2a^2$. Thus, the value of λ determining the tangent confocal conic is

$$\lambda = \frac{c^2 - (m^2a^2 + b^2)}{1+m^2}\,. \tag{4}$$

Notice that, because of Theorem 11, all the subsequent segments of the trajectory are tangent to the same conic, and the preceding reasoning applies to any of them. In other words, λ is a first integral of motion.

Thus, we have two known integrals, $I = \langle \mathbf{L}_1, \mathbf{L}_2 \rangle$ and a new one λ. They are not independent, though (again, the proof is a long but straightforward computation).

Proposition 12 *The integrals I and λ are related by*

$$\lambda = I - b^2\,.$$

4 Periodic orbits

In this section, following Sieber [10], we determine the conditions that a trajectory on an elliptic billiard must satisfy in order to be periodic (notice how this approach is different to the one used in previous works [3, 5] where periodic orbits are found by numerical brute force and trial and error, following a trajectory until it passes again through the intial point, within a certain tolerance). For notational reasons, we will introduce a rescaling of the invariant $I = \langle \mathbf{L}_1, \mathbf{L}_2 \rangle$ by the energy (which is also an invariant):

$$\alpha = \frac{I}{4E}\,. \tag{5}$$

Our main tool to determine periodic orbits is the Arnold-Liouville-Mineur theorem, and this requires computing the action coordinates of the elliptic billiard. As these are given by integrals of the momenta, and they turn out to be related to the first integrals of the system, it will be convenient to write the momenta in terms of the integrals E, α (we could as well take $E, I = L_1 L_2$, but the expressions in terms of E, α are cleaner, as we will see). Some long and boring computations lead to

$$p_\eta^2 = E(f^2 \sin^2\eta + \alpha)\,, \tag{6}$$

and

$$p_\xi^2 = E(f^2 \sinh^2\xi - \alpha)\,. \tag{7}$$

Now we are ready to build the action integrals. These are

$$I_\xi = \frac{1}{2\pi}\oint p_\xi \,\mathrm{d}\xi = \frac{\sqrt{E}}{\pi}\int_{\xi_0}^{\xi_1} \sqrt{f^2\sinh^2\xi - \alpha}\,\mathrm{d}\xi \tag{8}$$

$$I_\eta = \frac{1}{2\pi}\oint p_\eta \,\mathrm{d}\eta = \frac{2\sqrt{E}}{\pi}\int_{\eta_0}^{\eta_1} \sqrt{f^2\sin^2\eta + \alpha}\,\mathrm{d}\eta\,, \tag{9}$$

where the limits of integration are given by

- For $\alpha > 0$, $\xi_0 = \operatorname{asinh}\frac{\sqrt{|\alpha|}}{f}, \xi_1 = \operatorname{asinh}\frac{b}{f}, \eta_0 = 0, \eta_1 = \frac{\pi}{2}$.
- For $\alpha < 0$, $\xi_0 = 0, \xi_1 = \operatorname{asinh}\frac{b}{f}, \eta_0 = \arcsin\frac{\sqrt{|\alpha|}}{f}, \eta_1 = \frac{\pi}{2}$.

Not surprisingly at all, the integrals in (8) and (9) can be solved in terms of elliptic functions:

$$I_\xi = \begin{cases} \dfrac{\sqrt{E}}{\pi}\left[\dfrac{a}{b}\sqrt{b^2-\alpha} - \dfrac{f}{\kappa}E\left(\arcsin\sqrt{\dfrac{b^2-\alpha}{b^2}}, \kappa\right)\right] \\ \dfrac{\sqrt{E}}{\pi}\left[\dfrac{ab}{\sqrt{b^2-\alpha}} - \dfrac{\alpha}{f}F\left(\arcsin\sqrt{\dfrac{b^2}{b^2-\alpha}}, \dfrac{1}{\kappa}\right) - fE\left(\arcsin\sqrt{\dfrac{b^2}{b^2-\alpha}}, \dfrac{1}{\kappa}\right)\right] \end{cases},$$

(for $\alpha > 0$ and $\alpha < 0$, respectively) and

$$I_\eta = \begin{cases} \dfrac{2\sqrt{E}}{\pi}\dfrac{f}{\kappa}E\left(\kappa\right) \text{ , for } \alpha > 0 \\ \dfrac{2\sqrt{E}}{\pi}\left[\dfrac{\alpha}{f}K\left(\dfrac{1}{\kappa}\right) + fE\left(\dfrac{1}{\kappa}\right)\right] \text{ , for } \alpha < 0\,. \end{cases}$$

where the modulus is

$$\kappa = \frac{f}{\sqrt{f^2+\alpha}}\,,$$

and F, E denote, respectively, the elliptic incomplete integrals of the first and second kind, while K is the *complete* elliptic integral of the first kind.

The periodic orbits live on the tori given by the Arnold-Liouville-Mineur theorem, and in order to be closed trajectories on these tori, the quotient of the angular frequencies w_ξ, w_η must be rational. Thus, we have the condition that, for some $m, n \in \mathbb{N}$,

$$\frac{w_\xi}{w_\eta} = \frac{\left.\frac{\partial E}{\partial I_\xi}\right|_{I_\eta}}{\left.\frac{\partial E}{\partial I_\eta}\right|_{I_\xi}} = -\left.\frac{\partial I_\eta}{\partial i_\xi}\right|_E = -\frac{\left.\frac{\partial i_\eta}{\partial \alpha}\right|_E}{\left.\frac{\partial I_\xi}{\partial \alpha}\right|_E} = \frac{n}{m}\,, \tag{10}$$

where, by the properties of elliptic integrals,

$$\left.\frac{\partial I_\xi}{\partial \alpha}\right|_E = \begin{cases} -\dfrac{\sqrt{E}\kappa}{2\pi f} F\left(\arcsin\sqrt{\dfrac{b^2-\alpha}{b^2}}, \kappa\right) \text{, for } \alpha > 0 \\ -\dfrac{\sqrt{E}}{2\pi f} F\left(\arcsin\sqrt{\dfrac{b^2}{b^2-\alpha}}, \dfrac{1}{\kappa}\right) \text{, for } \alpha < 0\,, \end{cases}$$

and

$$\left.\frac{\partial I_\eta}{\partial \alpha}\right|_E = \begin{cases} \dfrac{\sqrt{E}\kappa}{\pi f} K(\kappa) \text{, for } \alpha > 0 \\ \dfrac{\sqrt{E}}{2\pi f} K\left(\frac{1}{\kappa}\right) \text{, for } \alpha < 0\,. \end{cases}$$

Two possibilities that can appear, depending on the sign of the invariant α. For instance, when $\alpha > 0$ (the case $\alpha < 0$ can be similarly analyzed) the condition for periodic orbits (10) reads

$$F\left(\arcsin\sqrt{\frac{b^2-\alpha}{b^2}}, \kappa\right) = \frac{2m}{n} K(\kappa)\,,$$

or, by applying elliptic inverses,

$$\sqrt{\frac{b^2-\alpha}{b^2}} = \mathrm{sn}\left(\frac{2m}{n} K(\kappa)\right)\,, \tag{11}$$

which has a solution for all $n \in \mathbb{N}, n \geq 3$, and $1 \leq m < n/2$. The integers n, m have the interpretation of number of rebounds of the orbit and its rotation number[5], respectively.

The values of κ (hence, α) that satisfies (11) must be determined numerically but, fortunately, there exist very fast and stable algorithms for dealing with elliptic functions.

[5]Roughly, how many times the trajectory makes a whole loop around.

4.1 Practical computations

Let us see how the knowledge of the first integral α (as numerically computed in (11)) determines the slope of the first segment of a closed orbit. We will make use of the invariant λ, which appeared in subsection 3.2. There, we saw that λ parameterizes a family of confocal ellipses in such a way that $\lambda = 0$ corresponds to the boundary ellipse of the billiard, and we could determine the value of λ corresponding to the confocal ellipse to which the first segment of a trajectory is tangent. If that segment belongs to the line $y = mx + c$, we found in (4) that

$$\lambda = \frac{c^2 - (m^2a^2 + b^2)}{1 + m^2}\,.$$

Suppose now we want to compute a closed $n-$orbit starting at a point (x_0, y_0) on the border of the billiard. Let $y = mx + c$ be the line containing its initial segment. As it starts at (x_0, y_0), we must have $y_0 = mx_0 + c$, or $c = y_0 - mx_0$. Substituting in the expression for λ above, we get a relation between the slope m and λ: $\lambda = ((y_0 - mx_0)^2 - (m^2a^2 + b^2))/(1 + m^2)$. Moreover, in Proposition 12 we found a relation between λ and the invariant I. Let us make the assumption that $E = 1/4$, for simplicity[6]. In this case, we have $\alpha = I$, and also $\lambda = \alpha - b^2$. By considering these expressions for λ together, we get a system of equations which leads to

$$\alpha = \frac{(y_0 - mx_0)^2 - m^2(a^2 - b^2)}{1 + m^2}\,.$$

This is the expression used in the Maxima code, but we can turn it into an explicit relation between m and α: First, write $(1+m^2)\alpha = (y_0 - mx_0)^2 - m^2(a^2 - b^2)$, then factor terms containing powers of m, $(\alpha + x_0^2 + a^2 - b^2)m^2 + 2x_0y_0m - y_0^2 = 0$, and finally get $m = \left(x_0y_0 \pm \sqrt{\alpha + a^2 - b^2 + 2x_0y_0}\right)/(\alpha + a^2 - b^2 + x_0^2)$.

Although the computations can be made simbollically, for large orbits this would cause a buffer overflow, hence the code converts everything to bfloats, thus introducing small rounding errors that, if so desired, can be avoided substituting the `bfloat` commands by `radcan` ones.

5 Simulations in a CAS

5.1 Elliptic billiards

The command `elliptic_billiard(a,b,xinit,yinit,phi0,N)` simulates the behavior of an elliptic billiard table, where `a,b` are the major and minor semiaxes of the bounding ellipse, `xinit,yinit` are the coordinates of the initial point (it can lay in the interior of the ellipse), `phi0` is the initial angle (measured counterclockwise in radians with respect to the horizontal), and the positive integer `N` is the number of rebounds.

Let us see some examples of their use:

```
(%i1) elliptic_billiard(4,3,2.5,1.13,0.7*%pi,50);
```

[6] That just means that we will be selecting a particular $n-$orbit among the many possible.

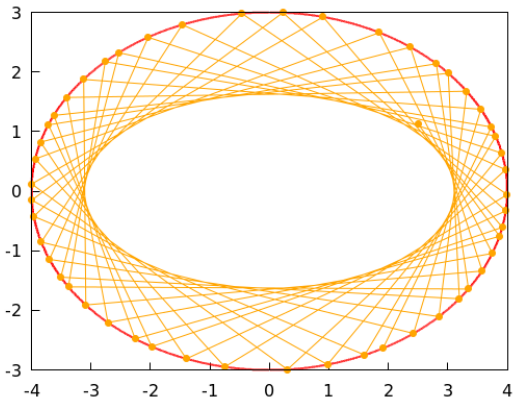

The same initial point but with a different initial slope:

```
(%i2) elliptic_billiard(4,3,2.5,1.13,%pi/3,50);
```

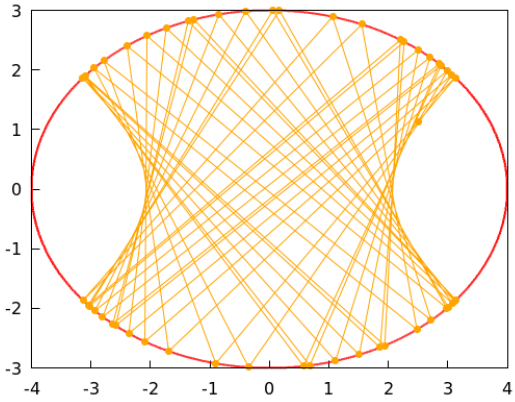

Here we see the degenerate case of a circular billiard:

```
(%i3) elliptic_billiard(2,2,4/9,4/9,0.469*%pi,50);
```

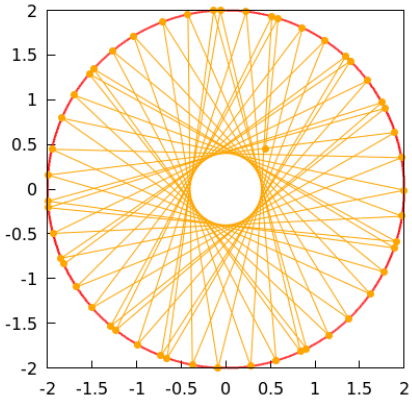

An animation of this last example can be produced with the previous command suitably modified:

```
(%i4) elliptic_billiard_animated(2,2,4/9,4/9,0.469*%pi,50);
```

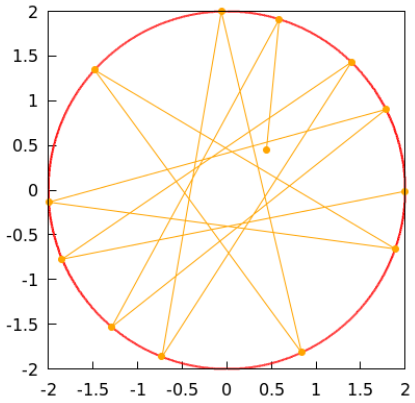

For the sake of completeness, let us comment on some of the computations required in the function `elliptic_billiard` (see Section 6). First, assume that we already know a point of impact with the boundary, (x_n, y_n), and the velocity after the rebound, (u_n, v_n), so we want to determine the next point of impact (x_{n+1}, v_{n+1}). The parametric equations of the line $\mathbf{r}(t)$ joining these two points are $r_1(t) = x_n + tu_n$ and $r_2(t) = y_n + tv_n$. This line meets the ellipse at two points, determined by the condition $r_1^2/a^2 + r_2^2/b^2 = (x_n + tu_n)^2/a^2 + (y_n + tv_n)^2/b^2 = 1$. Developing this expression and taking into account that (x_n, y_n) lies on the ellipse (so $x_n^2 + y_n^2 = 1$) we get

$$\left(\frac{2x_nu_n + tu_n^2}{a^2} + \frac{2ty_nv_n + tv_n^2}{b^2}\right) t = 0\,,$$

which has two solutions: $t = 0$ (corresponding to (x_n, y_n)), and the one of interest for us: $t = -2(x_nu_nb^2 + y_nv_na^2)/(b^2u_n^2 + a^2v_n^2)$. By substituting in the equations above, we find the coordinates of the point of intersection:

$$\begin{cases} x_{n+1} = x_n - 2\dfrac{x_nu_nb^2 + y_nv_na^2}{b^2u_n^2 + a^2v_n^2}u_n \\ y_{n+1} = y_n - 2\dfrac{x_nu_nb^2 + y_nv_na^2}{b^2u_n^2 + a^2v_n^2}v_n\,. \end{cases}$$

Next, we need to compute the velocity vector after the impact, (u_{n+1}, v_{n+1}). This vector is the reflection of the incoming velocity (u_n, v_n) across the normal line of the ellipse at (x_{n+1}, y_{n+1}). The inward normal[7] (N_1, N_2) is easily found:

$$(N_1, N_2) = -\frac{\left(\frac{2x_n}{a^2}, \frac{2y_n}{b^2}\right)}{\left\| \left(\frac{2x_n}{a^2}, \frac{2y_n}{b^2}\right) \right\|} = \frac{-1}{\sqrt{b^4x_{n+1}^2 + a^4y_{n+1}^2}}(b^2x_{n+1}, a^2y_{n+1})\,.$$

[7] We need to take the inward normal, so the ball bounces *into* the ellipse.

The reflection of (u_n, y_n) across the line determined by (x_{n+1}, y_{n+1}) and (N_1, N_2) is given by $(u_{n+1}, v_{n+1}) = (u_n, v_n) - 2\,\langle (u_n, v_n), (N_1, N_2)\rangle\,(N_1, N_2)$, which leads to the expressions used in the code (compare with [3]):

$$\begin{cases} u_{n+1} = u_n - \dfrac{2(b^2 x_{n+1} u_n + a^2 y_{n+1} v_n)}{b^4 x_{n+1}^2 + a^4 y_{n+1}^2} b^2 x_{n+1} \\ v_{n+1} = v_n - \dfrac{2(b^2 x_{n+1} u_n + a^2 y_{n+1} v_n)}{b^4 x_{n+1}^2 + a^4 y_{n+1}^2} a^2 y_{n+1} \,. \end{cases}$$

The preceding reasonings can *not* be applied to the first segment of the orbit, as (x_0, y_0) does not necessarily lie on the ellipse[8]. Thus, we start with the initial point (x_0, y_0) and the initial velocity, which is the unitary vector (u_0, v_0) along the direction given by the slope $m_0 = \tan\phi_0$, that is, $(u_0, v_0) = (1, \tan\phi_0)\,/\sqrt{1+\tan^2\phi_0}$ (the particular cases $\phi_0 = \pi/2$ and $\phi_0 = 3\pi/2$, for which (u_0, v_0) are $(0, 1)$ and $(0, -1)$, respectively, are treated separatedly).

We want an explicit formula for (x_1, y_1) depending on these data alone. The initial segment of the orbit is the line $y = m_0 x + c_0$, so $c_0 = y_0 - m_0 x_0$. Substitution into the ellipse's equation yields $(x/a)^2 + ((m_0 x + c_0)/b)^2 = 1$, so the x coordinate of the new point must satisfy $(b^2 + a^2 m_0^2)x^2 + 2a^2 m_0 c_0 x + a^2(c_0^2 - b^2) = 0$, a quadratic equation with two solutions, depending only on (a, b, m_0, c_0). Let us label them $x_+ \geq x_-$. A geometric interpretation of $y = m_0 x + c_0$ and the relative positions of $(x_0, y_0), (x_1, y_1)$, makes clear that we must choose x_+ when $u_0 > 0$ (so the line $y = m x_0 + c_0$ is traveled left to right and the abcissa x_1 is to the right of x_0), and choose x_- when $u_0 < 0$ (so the line $y = m x_0 + c_0$ is traveled right to left and the abcissa x_1 is to the left of x_0).

5.2 Periodic orbits

5.2.1 Case $I > 0$ (elliptic caustic)

The function is `norbits_elliptic(a,b,x0,N,m)`. Its syntax should be clear, the only caveat is that N represents the number of points in the orbit (number of bounces or rebounds), while m represents the rotation number (roughly speaking, how many times the closed orbit winds around), which must satisfy the restriction $m < N/2$. As the starting point is taken on the ellipse, only the initial coordinate `xinit` is needed (the corresponding `yinit` is determined from the ellipse equation). Here are some examples, starting with a $4-$orbit on an ellipse of semiaxes $a = 4$, $b = 3$, and rotation number $N = 1$ (the initial point is taken at $x_0 = 1.3$):

```
(%i5) norbits_elliptic(4,3,1.3,4,1);
```

[8] In the formulae for (u_{n+1}, v_{n+1}) we use the expressions for (x_{n+1}, y_{n+1}), which were obtained under the assumption that (x_n, y_n) was on the ellipse.

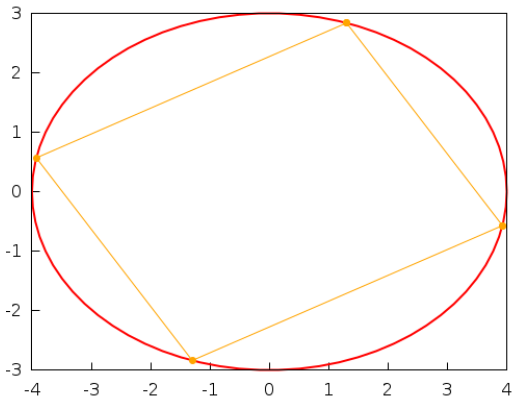


```
(%i6) norbits_elliptic(4,3,2.25,11,3);
```

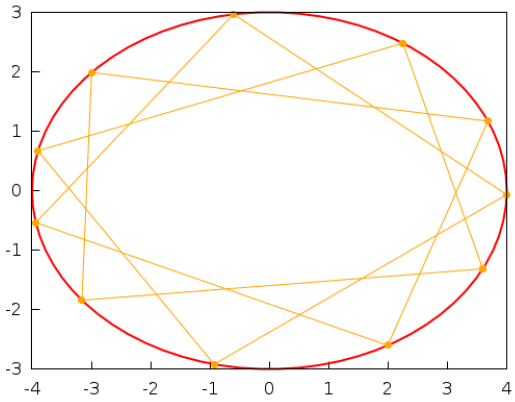


```
(%i7) norbits_elliptic(4,3,1.3,35,6);
```

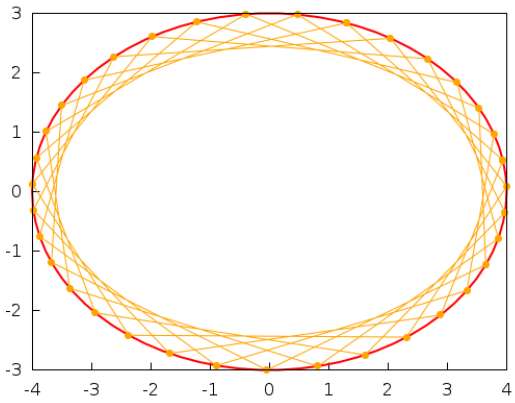

5.2.2 Case $I < 0$ (hyperbolic caustic)

The command and syntax are completely analogous to the previous one. It will suffice to give an example of its use:

```
(%i8) norbits_hyperbolic(5,3,1.28,4,1);
```

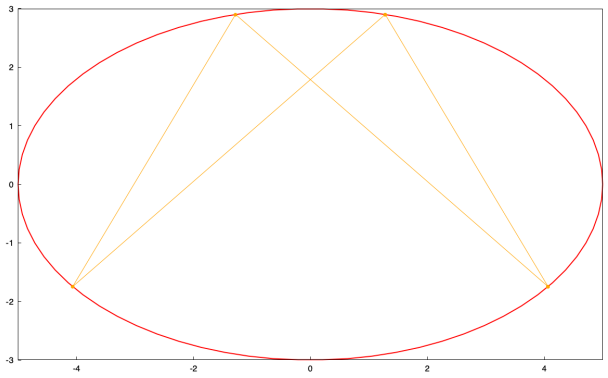

As a particular feature of this case, there are some conditions that must be satisfied in order to get an orbit. If that does not occur, a message will be issued.

```
(%i9) norbits_hyperbolic(4,3,1.28,6,1);
(%o9) With these parameters, the motion takes place on a complex
torus. Please, select them so the condition b/a<sin(m*%pi/N) is
satisfied
```

5.3 Poincaré sections

It is also possible to analyze Poincaré sections nof elliptic billiards, which are the basic tool to study the onset of chaos in a dynamical system [9],[12]. This is done by the function below, whose arguments are the semiaxes a, b, a list of initial conditions of the form $[[\theta_0, \phi_0], \ldots, [\theta_k, \phi_k]]$ (such that the initial point on the ellipse is $(x_0, y_0) = (a\cos\theta_0, b\sin\theta_0)$ and the slope of the initial trajectory is $m_0 = \tan\phi_0$), and the number of iterations N. As an example, with the following command we compute the Poincaré section of an elliptic billiard of semi-axes $a = 4$, $b = 3$, following the trajectories of 11 points given by initial conditions of the form $[\theta_j, \phi_j] = [\pi/3, -\pi + 2\pi j/10]$, along 100 rebounds:

```
(%i10) eb_poincare(4,3,makelist([%pi/3,-%pi+2*j*%pi/10],j,0,10),100);
```

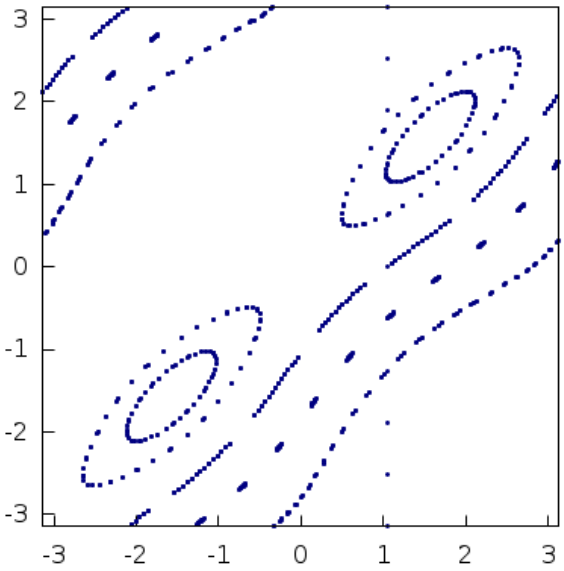

Notice how these Poincaré sections are, basically, deformations of that of a harmonic oscillator, reflecting the integrability of elliptic billiards.

6 Code example

As an example of the practical implementation of the ideas exposed in the paper, here is the code of the Maxima function `elliptic_billiard` and the auxilliary `norbits_elliptic_angle` used to simulate the behavior of an elliptic billiard table. The syntax is

```
elliptic_billiard(a,b,xinit,yinit,phi0,N)
```

where `a,b` are the major and minor semiaxes of the bounding ellipse, `xinit,yinit` are the coordinates of the initial point (it can lay in the interior of the ellipse), `phi0` is the initial angle (measured counterclockwise in radians with respect to the horizontal), and the positive integer `N` is the number of rebounds.

```
(%i1)      norbits_elliptic_angle(a,b,N,m):=block(
           [foc:sqrt(a^2-b^2),eeqqnn,xx],
           if is(m>=N/2) then
               return("The rotation number must satisfy m<N/2"),
           eeqqnn:bfloat(sqrt(b^2-xx)/(b)-jacobi_sn((2*m/N)*elliptic_kc(foc^2/(foc^2+xx)),foc^2/(foc^2+xx))),
           bf_find_root(eeqqnn,xx,0.001,b^2)
           )$
```

```
(%i2)     elliptic_billiard(a,b,xinit,yinit,phi0,N):=
          block(
          [ratprint:false,solns,xp,xm,segments],
          local(x,y,u,v,m,c),
          if is(a<b) then
              return("The semiaxes must satisfy b<a"),
          if (is(not(integerp(N))) or is(N<1)) then
              return("The number of rebounds must be a positive integer"),
          if is(bfloat((xinit/a)^2+(yinit/b)^2-1)>0) then
              return("The initial point does not lie on the ellipse or its interior"),
          if (is(phi0=%pi/2) or is(phi0=0.5*%pi))
              then (x[0]:bfloat(xinit),y[0]:bfloat(yinit),
              x[1]:x[0],y[1]:b*sqrt(1-(x[1]/a)^2),u[0]:0,v[0]:1)
          elseif (is(phi0=3*%pi/2) or is(phi0=1.5*%pi))
              then (x[0]:bfloat(xinit),y[0]:bfloat(yinit),
              x[1]:x[0],y[1]:-b*sqrt(1-(x[1]/a)^2),u[0]:0,v[0]:-1)
          else (
          m[0]:bfloat(tan(phi0)),
          x[0]:bfloat(xinit),
          y[0]:bfloat(yinit),
          u[0]:1/sqrt(1+(m[0])^2),
          v[0]:m[0]/sqrt(1+(m[0])^2),
          c[0]:y[0]-m[0]*x[0],
          solns:bfloat(map('rhs,solve(
          (b^2+a^2*(m[0])^2)*x^2+2*a^2*m[0]*c[0]*x+a^2*((c[0])^2-b^2),x))),
          xp:lmax(solns),
          xm:lmin(solns),
          if is(u[0]<0) then x[1]:xm
          elseif is(u[0]>0) then x[1]:xp,
          y[1]:m[0]*x[1]+c[0]
              ),
          u[1]:u[0]-2*(b^2*x[1]*u[0]+a^2*y[1]*v[0])*b^2*x[1]/(b^4*(x[1])^2+a^4*(y[1])^2),
          v[1]:v[0]-2*(b^2*x[1]*u[0]+a^2*y[1]*v[0])*a^2*y[1]/(b^4*(x[1])^2+a^4*(y[1])^2),
          for j:1 thru N do (
          x[j+1]:x[j]-2*(x[j]*u[j]*b^2+y[j]*v[j]*a^2)*u[j]/(b^2*(u[j])^2+a^2*(v[j])^2),
          y[j+1]:y[j]-2*(x[j]*u[j]*b^2+y[j]*v[j]*a^2)*v[j]/(b^2*(u[j])^2+a^2*(v[j])^2),
          u[j+1]:u[j]
          -2*(b^2*x[j+1]*u[j]+a^2*y[j+1]*v[j])*b^2*x[j+1]/(b^4*(x[j+1])^2+a^4*(y[j+1])^2),
          v[j+1]:v[j]
          -2*(b^2*x[j+1]*u[j]+a^2*y[j+1]*v[j])*a^2*y[j+1]/(b^4*(x[j+1])^2+a^4*(y[j+1])^2)
          ),
          segments:makelist([x[j],y[j]],j,0,N),
          wxdraw2d(proportional_axes=xy,
          color=red,line_width=2,nticks=75,
          parametric(a*cos(t),b*sin(t),t,0,2*%pi),
          color=orange,line_width=1,
          points_joined=true,
          point_type=filled_circle,
          points(segments))
          )$
```


Acknowledgements

The author express his gratitude to Prof. Aldo Boiti for many useful suggestions and detailed comments on the contents of this paper.

References

[1] V. I. ARNOLD, *Mathematical methods of classical mechanics*, vol. 60 of Graduate Texts in

Mathematics, Springer-Verlag New York, 1989.

[2] G. BIRKHOFF, *Dynamical Systems*, AMS publishing, Providence, USA, 1927.

[3] A. BOITI, *Exact Orbits of Light Rays Reflected Inside Ellipses, Traced by Means of Rational Formulae with the Help of the CAS Derive™ 6*, The Electronic Journal of Mathematics and Technology, 17-2 (2023), pp. 125 – 137.

[4] G. CASATI, B. V. CHIRIKOV, AND J. FORD, *Marginal local instability of quasi-periodic motion*, Physics Letters A, 77 (1980), pp. 91 – 94.

[5] G. DÁVILA-RASCÓN AND W.C. YANG, *Investigating the Reflections of Light Rays Inside Ellipses with GeoGebra, Maxima and Maple*, The Electronic Journal of Mathematics and Technology, 13-3 (2020), pp. 190 – 218.

[6] L. HALBEISEN AND N. HUNGERBÜHLER, *A simple proof of Poncelet's theorem (on the occasion of its bicentennial)*, The American Mathematical Monthly, 122 (2015), pp. 537–551.

[7] V. V. KOZLOV AND D. V. TRESHCHEV, *Billiards: A Genetic Introduction to the Dynamics of Systems with Impacts*, vol. 89 of Translations of Mathematical Monographs, American Mathematical Society, 1991.

[8] J. MASOLIVER AND A. ROS, *Integrability and chaos: the classical uncertainty*, European Journal of Physics 32 2 (2011) 431–458.

[9] E. OTT, *Chaos in Dynamical Systems*, Cambridge University Press, 2 ed., 2002.

[10] M. SIEBER, *Semiclassical transition from an elliptical to an oval billiard*, Journal of Physics A: Mathematical and General, 30 (1997) 4563–4596.

[11] I. G. SINAI, *Introduction to Ergodic Theory*, Princeton University Press, 1977.

[12] S. STROGATZ, *Nonlinear Dynamics and Chaos*, CRC Press, 2 ed., 2015.

[13] S. TABACHNIKOV, *Geometry and Billiards*, vol. 30 of Student Mathematical Library, American Mathematical Society, 2005.